Geophys. J. Int. (2000) **143,** 119–128

Constraints on a plume in the mid-mantle beneath the Iceland region from seismic array data

M. J. Pritchard,[1] G. R. Foulger,[1] B. R. Julian[2] and J. Fyen[3]

[1] *Department of Geological Sciences, University of Durham, South Road, Durham* DH1 3LE, *UK. E-mail: g.r.foulger@durham.ac.uk*
[2] *US Geological Survey,* 345 *Middlefield Rd, Menlo Park,* CA 94025, *USA*
[3] *NORSAR,* PO Box 51, N-2007 *Kjeller, Norway*

Accepted 2000 May 4. Received 2000 May 4; in original form 1998 December 15

SUMMARY

Teleseismic *P* waves passing through low-wave-speed bodies in the mantle are refracted, causing anomalies in their propagation directions that can be measured by seismometer arrays. Waves from earthquakes in the eastern Pacific and western North America arriving at the NORSAR array in Norway and at seismic stations in Scotland pass beneath the Iceland region at depths of ~1000–2000 km. Waves arriving at NORSAR have anomalous arrival azimuths consistent with a low-wave-speed body at a depth of ~1500 km beneath the Iceland–Faeroe ridge with a maximum diameter of ~250 km and a maximum wave-speed contrast of ~1.5 per cent. This agrees well with whole-mantle tomography results, which image a low-wave-speed body at this location with a diameter of ~500 km and a wave-speed anomaly of ~0.5 per cent, bearing in mind that whole-mantle tomography, because of its limited resolution, broadens and weakens small anomalies. The observations cannot resolve the location of the body, and the anomaly could be caused in whole or in part by larger bodies farther away, for example by a body imaged beneath Greenland by whole-mantle tomography.

Key words: array, Iceland, mantle, plume, seismology.

INTRODUCTION

Morgan (1971) proposed that convective plumes rising from the lower mantle underlie 'hotspots' such as Hawaii and Iceland. There is considerable evidence for large volumes of anomalously hot, partially molten material beneath hotspots in the upper mantle. However, the lower mantle is more difficult to study, because of its great depth, and there is thus weaker evidence constraining the presence or absence of plumes there.

Recent whole-mantle tomography has shown large-scale structures that traverse the whole mantle in some regions. Zones a few hundred kilometres wide and tens of thousands of kilometres long, with *P*-wave speeds $V_P \sim 0.5$ per cent high, extend into the lower mantle beneath some, though not all, regions where subduction has occurred during the past 180 Myr (e.g. van der Hilst *et al.* 1997; Megnin & Romanowicz 2000). Fewer zones of low wave speed extending throughout the whole mantle have been observed, but one clear example is a continuous zone that extends from the core–mantle boundary beneath the south Atlantic ocean to the surface beneath east Africa (Ritsema *et al*. 1999). The presence of such a continuous low-wave-speed zone beneath a hotspot does not necessarily indicate a zone of upwelling traversing the whole mantle, however, because coupled, two-layer convection may occur. Evidence has been presented for the association of hotspots with substantial, lower mantle anomalies from analysis of geoid highs and by dynamic plume modelling. For example, Richards *et al.* (1988) present evidence that the major low-density anomalies causing the geoid highs associated with hotspots are in the lower mantle.

A few studies have specifically focused on seeking narrow, cylindrical, low-wave-speed anomalies in the lower mantle. The Hawaii hotspot was investigated by Ji & Nataf (1998), who applied 2-D waveform tomography to scattered long-period *P* waves in a search for vertical, cylindrical structures in the lowest 1000 km of the mantle. In an area ~200 km northwest of Hawaii they found a double feature which they suggested indicated two plumes in a region assumed to be 250 km broad. The strength of this feature is considerably greater than the expected effect of a 600 K thermal anomaly, presenting difficulties in physical interpretation and bringing into question the result. Nataf & VanDecar (1993) studied the Bowie hotspot by applying cross-correlation techniques to seismic data from Alaskan earthquakes recorded on a 120-station network in Washington state, USA. They found a traveltime delay of 0.15 s for *P* waves passing subhorizontally beneath the Bowie hotspot at a depth of about 700 km. This they interpreted as indicating a 150 km wide low-wave-speed plume conduit with an inferred temperature anomaly of about 300 K.

The Iceland hotspot is one of the best-studied hotspots in the world, because it is large, overlain by an extensive landmass, flanked by cratons at moderate distances, and attracts scientific

investigation because it is by far the most extensive example of subaerial spreading. Teleseismic tomography and attenuation studies reveal a low-wave-speed body in the uppermost ~400 km with a diameter of ~250 km and anomalies of up to ~3 per cent in V_P and 5 per cent in V_S (Tryggvason *et al.* 1983; Wolfe *et al.* 1997; Allen *et al.* 1998; Foulger *et al.* 2000). Such anomalies correspond to a temperature variation of up to 200–250 K. The high-resolution image of Foulger *et al.* (2000) reveals a morphological change from axial symmetry to tabular symmetry starting at ~250 km depth, which was interpreted as evidence that hot material beneath Iceland rises from the transition zone in the lowermost upper mantle.

The conclusion, that the buoyant upwelling beneath Iceland is restricted to the upper mantle, is supported by the results of several recent, whole-mantle seismic tomography experiments that have provided high-quality images of mantle structure beneath Iceland (Bijwaard & Spakman 1999; Bijwaard *et al.* 1998; Ritsema *et al.* 1999; Megnin & Romanowicz 2000). These studies all agree that the north Atlantic at the latitude of Iceland is underlain by a major low-wave-speed anomaly with a strength of a few per cent in the upper mantle. Structure in the lower mantle beneath is radically different, however, and wave speeds there are everywhere within ~0.5 per cent of normal. Bijwaard & Spakman (1999) found a continuous, weak (<0.5 per cent) low-wave-speed body in the lower mantle that extends from the core–mantle boundary beneath the Iceland–Greenland ridge to the mantle transition zone beneath the Iceland–Faeroe ridge. It is continuous with the strong, upper mantle body at a location 250 km southeast of Iceland. At ~700–1500 km depth beneath the Iceland–Faeroe ridge, this body is ~500 km in diameter and has a V_P anomaly of up to ~0.5 per cent. Its dimensions are near the resolution limit of the study, so it could actually be smaller.

In a search for evidence for a plume in the lower mantle, Shen *et al.* (1996, 1998) used receiver functions to study the transition zone discontinuities near 400 and 650 km depths beneath Iceland. They found that the 400 km discontinuity is deeper than average, and that the 650 km discontinuity is shallower, in this region, with the distance between them smaller by as much as 20 km compared with surrounding areas. They interpreted this observation as evidence that a plume arises in the lower mantle and convects through both discontinuities. They estimated the associated temperature anomaly to be ~150 K, in good agreement with interpretations of the upper mantle teleseismic tomography results. Supporting evidence was presented by Helmberger *et al.* (1998), who modelled the interference of shear waves transmitted through, and refracted at, the core–mantle boundary beneath the Iceland region. They found evidence for a localized patch of ultra-low-wave-speed material in a dome 250 km wide and 40 km high at the core–mantle boundary. They interpreted this as a zone of partial melt that might be the source of a plume beneath Iceland.

In summary, seismic studies using diverse techniques to focus on specific localities beneath Iceland report observations consistent with a plume that arises from the core–mantle boundary and passes continuously through the 650 km and 400 km discontinuities as a vertical cylinder. Seismic tomography, on the other hand, consistently supports a model of a broad, strong anomaly in the upper mantle beneath Iceland and a much weaker structure, if any, in the lower mantle. The most optimistic interpretation of the tomographic images of the lower mantle suggests a large-scale, weak feature that is not vertically continuous with the upper mantle body beneath Iceland. Varying conclusions may also be derived from geochemistry. For example, the Nb/Y and Zr/Y ratios in surface rocks in the north Atlantic volcanic province suggest that most of the erupted material originated from the thermal boundary layer at the base of the upper mantle (Fitton *et al.* 1997). On the other hand, He^3/He^4 ratios in Iceland are the highest measured anywhere on Earth. Such high ratios are generally assumed to indicate material of lower mantle origin, although such an interpretation is currently under review (e.g. Anderson 1993, 1998a,b). It has been suggested that a plume originating from the lower mantle could entrain large volumes of upper mantle material, or that a plume arising from the mantle transition zone could draw up small amounts of lower mantle material in its core (Fitton *et al.* 1997). Thus, both the seismological and the geochemical observations are, to some extent, ambiguous or can be made to fit the desired model.

In this paper, we study azimuth-slowness anomalies to look for the seismic signature of a plume at depths of 1000–2000 km beneath the Iceland region. Such azimuth-slowness anomaly characterization is routinely underway as part of the Comprehensive Test Ban Treaty monitoring (Bondar *et al.* 1999). We use the directions of propagation of teleseismic *P* waves measured at a seismic array in Norway and a network of stations in Scotland. A weak signal consistent with a low-wave-speed body at ~1500 km depth beneath the Iceland–Faeroe ridge southeast of Iceland is found in the data from Norway, although the interpretation is not unique and a larger, deeper, low-wave-speed body beneath Greenland could also account for the observations. The data from Scotland are too noisy to detect this feature reliably. We place an upper bound on the dimensions and magnitude of the V_P anomaly that such a feature could have.

THE NORSAR ARRAY AND THE SCOTTISH NETWORK

The 100 km aperture Norwegian Seismic Array (NORSAR) in southern Norway (Fig. 1) was operated from the 1960s to the 1980s to study the problems of detecting and identifying nuclear explosions. The primary goal of NORSAR and similar arrays was to improve signal-to-noise ratios, by combining the outputs from individual sensors so that desired signals constructively interfered and noise did not. As a by-product, these arrays made it possible to measure directly the arrival directions (slowness vectors) of seismic waves. Such measurements usually differ substantially from the directions predicted from standard tables because of lateral variations in the Earth's structure. At NORSAR, *P* waves from earthquakes throughout the world were found to have slowness vectors systematically displaced eastwards by about 1 s deg^{-1}. This bias was attributed to structure in the crust and/or upper mantle directly beneath the array, which has a similar effect on waves from all directions (Sheppard 1973). On the other hand, there are found to be rapidly varying anomalies in slowness for earthquakes from some regions of the world, and the causes of such features must lie far from the array.

The most rapid variation in *P*-wave slowness anomaly at NORSAR occurs for earthquakes in middle America, whose waves approach from the west and northwest (Sheppard 1973). This anomaly was originally attributed to structure in the upper mantle beneath the earthquakes. However, waves from these

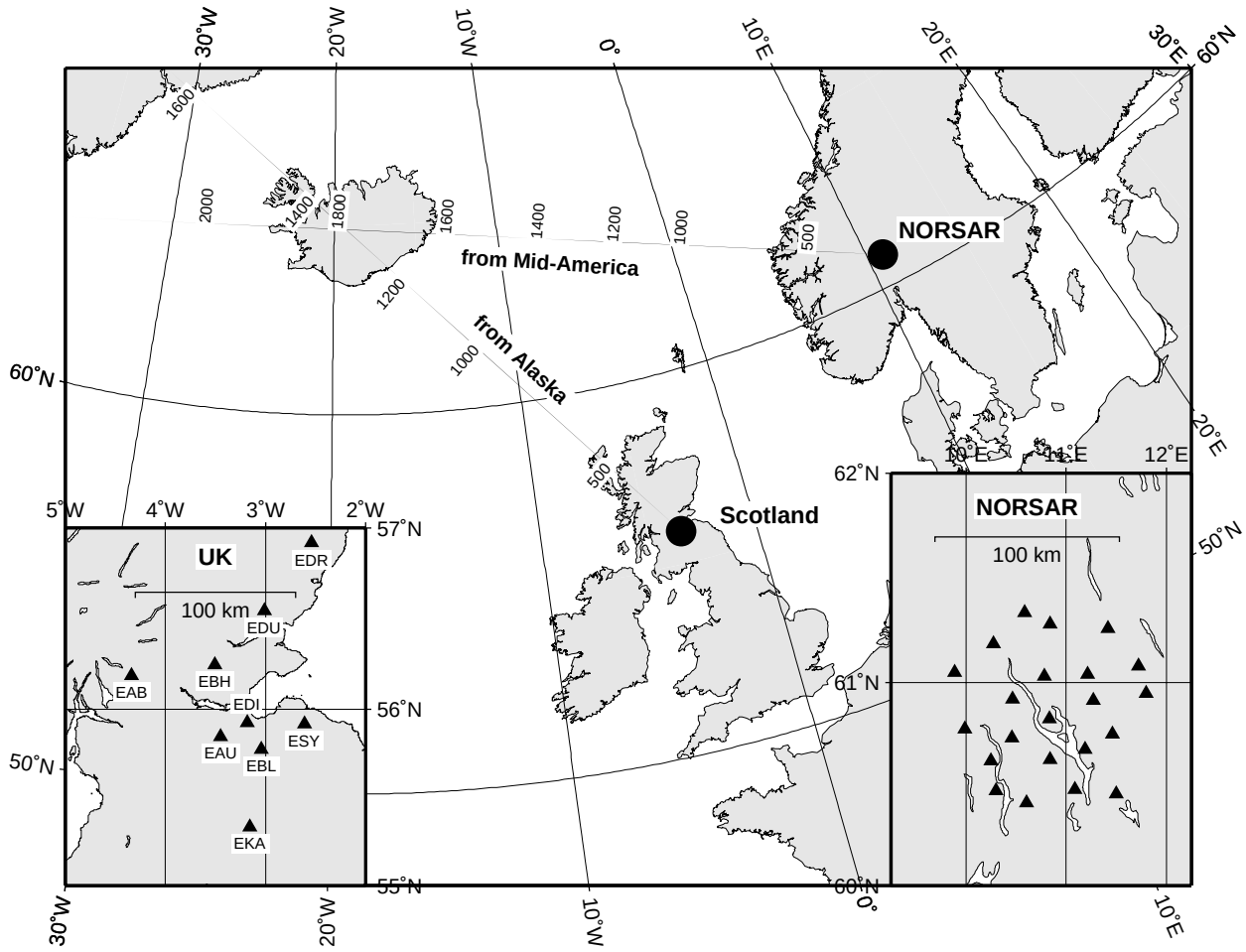

Figure 1. Map showing the NORSAR array and the seismic network in Scotland used in this study. Triangles in insets show locations of seismic stations (Scotland) and subarray centres (NORSAR). Lines show great circles along which waves passing beneath Iceland approach, with numbers indicating the depths, in km, of rays from typical epicentral distances (70° for the Scottish stations; 85° for NORSAR).

directions also pass beneath the Iceland region at a distance of ~1000–2000 km from NORSAR, raising the intriguing possibility that the anomaly might be related to structure in the lower mantle associated with the Iceland hotspot. If seismic waves pass near a low-wave-speed body, the first arrivals will be refracted around the body, and the range of azimuths observed at the array will be greater than the range of great-circle azimuths to the epicentres. Just such a distortion was noticed in the NORSAR data by Sheppard (1973).

Data from a single array can provide information on the direction of an anomalous structure, but place only weak constraints on its distance. In order to address this problem, we also analysed data from a network in southern Scotland in an attempt to fix the location of the causative body by triangulation.

DATA

Experimental geometry

The data used in this study consist of teleseismic *P*-wave arrival times measured from vertical-component seismograms recorded on the NORSAR array in southern Norway, and a group of stations in southern Scotland (Fig. 1). Both are located within 15° of Iceland. *P*-waves from teleseisms at epicentral distances between 70° (earthquakes in Alaska observed in Scotland) and 85° (earthquakes in middle America observed at NORSAR) pass through the mantle beneath the Iceland region at depths of ~1000–2000 km.

Data from NORSAR

We measured teleseisms from central America with array-to-event azimuths in the range 260°–320° that were recorded during 1973–1976 (Fig. 2). During this period, NORSAR consisted of 22 six-station subarrays, had an aperture of about 100 km, and could resolve slowness to within ~0.06 s deg^{-1}, or 0.6° in azimuth. All the stations had identical, vertical, short-period Hall-Sears HS-10-1/ARPA seismometers (Bungum *et al.* 1971). The data were digitized at each subarray at a sampling rate of 20 sps and transmitted to the main data processing centre by telephone line.

We extracted seismograms from a selection of the largest events (Table 1) from the archive of digital data on magnetic tape at the NORSAR data processing centre. We filtered them digitally with a passband of 0.5–2.0 Hz and measured the *P*-wave arrival-time differences at each sensor for the first coherent peak or trough. This amounts to picking an arrival about a quarter of a wavelength, or 0.25 s, after the first arrival,

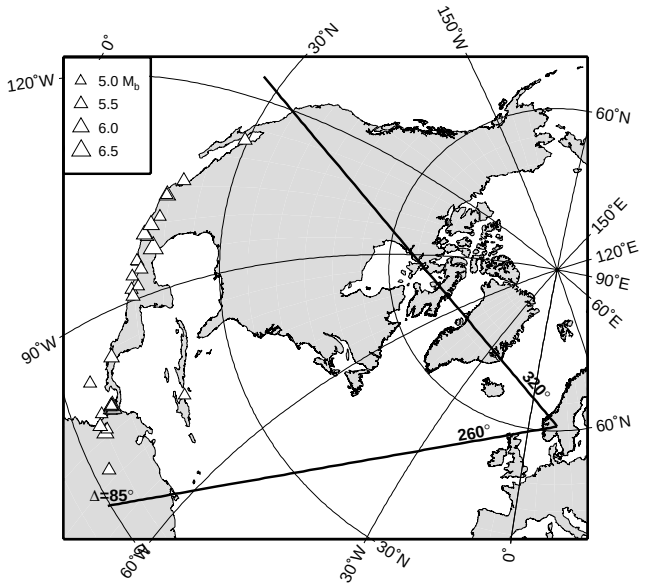

Figure 2. Map showing events used in this study, recorded at NORSAR during 1973–1976. The lines shown bound the array-to-event azimuth range 260°–320°. The typical epicentral distance is 85°.

and raises the possibility that the times may be affected by later arrivals, which have perhaps passed through the centre of the hypothesized plume, and interfere with the first arrival. Such an effect might introduce small errors into the anomaly we seek. However, the first breaks were often so emergent that the benefit-to-cost ratio of adopting our approach was high. We found that numerical cross-correlation was prone to cycle-skipping, and required all picks to be re-checked by hand and often re-picked visually. For this reason we used visual picks for the whole data set. We picked an arrival from at least one sensor in each subarray for each event wherever possible. Typically, about 20 of the 22 subarrays provided reliable picks.

Data from Scotland

No array of the aperture of NORSAR is available in the UK, the Eskdalemuir, Scotland array being only 20×20 km in size. Azimuth anomalies measured using such an array would have errors of $\sim 3^\circ$, and would thus be insufficiently accurate for this study. We therefore used as an array a subset of the seismic network operated by the British Geological Survey (BGS) in Scotland (Fig. 1).

Stations of the Scottish network have vertical, short-period, Wilmore Mk II/III seismometers, and data are relayed by

Table 1. Events recorded at NORSAR. The data are taken from the ISC bulletin.

Lat.	Long.	d (km)	Date	Origin time	M_b	(°)	Region
5.23°N	75.82°W	110	1973/04/24	18 : 42 : 31.5	5.3	83.8	COLOMBIA
19.97°N	73.05°W	24	1973/08/03	15 : 44 : 25.5	5.2	69.7	HAITI REGION
18.26°N	96.58°W	75	1973/08/28	09 : 50 : 39.1	6.6	82.2	VERA CRUZ, MEXICO
5.27°N	78.08°W	30	1973/09/16	08 : 21 : 37.9	5.3	84.9	SOUTH OF PANAMA
19.42°N	104.98°W	56	1973/10/18	10 : 49 : 39.3	6.0	84.8	NEAR COAST OF JALISCO, MEXICO
9.51°N	83.95°W	34	1974/02/28	20 : 20 : 10.4	5.8	84.0	COSTA RICA
14.52°N	91.64°W	106	1974/04/10	22 : 43 : 00.5	5.4	83.3	GUATEMALA
15.61°N	95.26°W	33	1974/06/25	05 : 01 : 01.2	5.2	84.0	NEAR COAST OF OAXACA, MEXICO
15.54°N	95.33°W	23	1974/06/25	08 : 44 : 45.3	5.4	84.1	NEAR COAST OF OAXACA, MEXICO
7.51°N	77.50°W	54	1974/07/13	02 : 20 : 24.6	5.5	82.6	PANAMA-COLOMBIA BORDER REGION
7.24°N	77.55°W	23	1974/07/13	23 : 08 : 42.6	5.3	82.9	PANAMA-COLOMBIA BORDER REGION
17.06°N	98.42°W	63	1974/07/18	19 : 21 : 26.3	5.5	84.1	GUERRERO, MEXICO
4.32°N	76.84°W	91	1974/08/24	02 : 47 : 31.1	5.7	85.1	COLOMBIA
2.72°N	71.37°W	44	1974/09/27	04 : 09 : 01.6	5.5	83.8	COLOMBIA
7.18°N	77.76°W	40	1975/01/25	02 : 08 : 41.8	6.0	83.1	PANAMA-COLOMBIA BORDER REGION
15.68°N	91.72°W	226	1975/02/03	01 : 03 : 26.6	5.3	82.3	MEXICO-GUATEMALA BORDER REGION
16.47°N	98.86°W	17	1975/04/23	11 : 14 : 49.3	5.9	84.8	NEAR COAST OF GUERRERO, MEXICO
29.49°N	113.40°W	30	1975/07/08	09 : 37 : 28.9	5.6	79.0	GULF OF CALIFORNIA
16.24°N	94.07°W	79	1975/08/19	14 : 57 : 11.6	5.6	82.9	OAXACA, MEXICO
14.65°N	93.48°W	15	1975/08/22	23 : 08 : 14.2	5.2	84.0	NEAR COAST OF CHIAPAS, MEXICO
6.96°N	77.67°W	27	1975/08/25	03 : 57 : 18.1	5.2	83.2	NEAR WEST COAST OF COLOMBIA
7.55°N	77.50°W	0	1975/11/21	01 : 14 : 55.6	5.8	82.6	PANAMA-COLOMBIA BORDER REGION
14.70°N	90.63°W	27	1976/02/06	18 : 19 : 21.4	5.6	82.7	GUATEMALA
21.63°N	106.60°W	43	1976/02/09	21 : 29 : 57.0	5.6	83.5	OFF COAST OF CENTRAL MEXICO
17.45°N	100.65°W	48	1976/06/07	14 : 26 : 39.9	6.0	84.7	GUERRERO, MEXICO
7.41°N	78.04°W	3	1976/07/11	20 : 41 : 47.9	6.1	83.0	PANAMA
7.06°N	78.15°W	37	1976/07/11	20 : 58 : 24.3	5.4	83.3	PANAMA
7.24°N	78.29°W	15	1976/07/12	14 : 43 : 08.6	5.4	83.3	PANAMA
7.42°N	78.02°W	16	1976/07/13	01 : 26 : 07.3	5.2	83.0	PANAMA
7.41°N	78.01°W	27	1976/07/14	01 : 32 : 34.6	5.4	83.0	PANAMA
7.41°N	78.11°W	43	1976/07/15	00 : 35 : 33.6	5.3	83.0	PANAMA
19.35°N	104.67°W	69	1976/07/17	09 : 02 : 14.7	5.2	84.8	NEAR COAST OF JALISCO, MEXICO
4.93°N	82.59°W	33	1976/07/24	10 : 43 : 22.5	5.4	87.4	SOUTH OF PANAMA
18.81°N	101.06°W	93	1976/09/05	20 : 11 : 39.2	5.3	83.7	GUERRERO, MEXICO

frequency-modulated analogue telemetry to Edinburgh. BGS personnel measure *P*-wave arrival times from paper playouts (D. Galloway, personal communication 1998) and report them to the International Seismological Centre (ISC), which publishes them in monthly Bulletins and distributes them in computer-readable form. We selected a group of stations covering an area similar to that of NORSAR for this analysis, and extracted *P*-wave arrival times from the ISC CD-ROMs for the period 1984–1994. We used teleseisms in the region from Vancouver Island through Alaska to the Aleutian Islands, which had event azimuths in the range 300°–360° (Fig. 3, Table 2).

Analysis of arrival times

We examined the arrival times for each event and rejected ~20 per cent of the data as outliers. Data were rejected if the relative observed arrival time (the arrival time minus the mean arrival time for the event) differed by more than 0.78 s from the value computed by applying the computer program of Buland & Chapman (1983) to the IASP91 Earth model (Kennett & Engdahl 1991). Events with fewer than four reliable arrival times were rejected, because this is the minimum number that provides redundancy in a plane-wave fit. Table 3 gives statistics for the data sets assembled.

For each event we fitted a plane wave by least-squares to the relative arrival times to obtain the horizontal slowness vector **p**. Because we used different subsets of stations for different events,

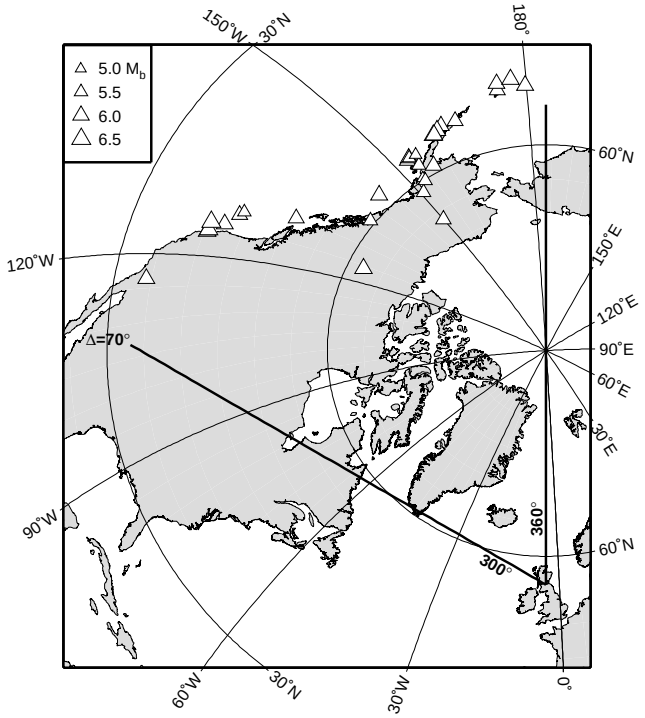

Figure 3. Map showing events used in this study, recorded at Scottish seismic stations during 1984–1994. The lines shown bound the network-to-event azimuth range 300°–360°. The typical epicentral distance is 70°.

Table 2. Events recorded in Scotland. The data are taken from the ISC bulletin.

Lat.	Long.	*d* (km)	Date	Origin time	M_b	(°)	Region
66.22°N	149.98°W	12	1985/03/09	14:08:04	5.8	55.4	ALASKA
43.50°N	127.62°W	10	1985/03/13	19:34:57	5.9	70.1	OFF COAST OF OREGON
62.19°N	124.27°W	6	1985/12/23	05:16:03	6.2	53.3	NORTH-WEST TERRITORIES, CANADA
51.42°N	174.84°W	5	1986/05/07	20:43:28	5.9	72.5	ANDREANOF ISLANDS, ALEUTIAN IS.
56.39°N	152.86°W	17	1986/06/19	09:09:10	5.9	65.1	KODIAK ISLAND REGION
56.19°N	153.40°W	31	1986/09/12	23:57:15	6.0	65.3	KODIAK ISLAND REGION
61.45°N	150.85°W	60	1987/04/18	02:01:37	5.7	59.9	SOUTHERN ALASKA
51.26°N	179.88°W	26	1987/05/06	04:06:15	6.1	72.9	ANDREANOF ISLANDS, ALEUTIAN IS.
54.20°N	162.66°W	33	1987/06/21	05:46:10	6.0	68.6	ALASKA PENINSULA
56.19°N	153.69°W	33	1987/07/24	05:25:11	5.5	65.4	KODIAK ISLAND REGION
57.74°N	142.94°W	10	1988/03/06	23:14:36	6.1	61.8	GULF OF ALASKA
54.29°N	165.58°W	104	1989/05/19	02:21:56	5.9	68.9	FOX ISLANDS, ALEUTIAN ISLANDS
57.80°N	154.29°W	43	1989/06/16	10:51:17	5.6	64.0	KODIAK ISLAND REGION
58.85°N	156.83°W	210	1990/05/01	16:12:21	6.0	63.3	ALASKA PENINSULA
59.34°N	136.67°W	10	1990/07/11	15:14:03	5.7	59.0	SOUTH-EASTERN ALASKA
54.59°N	161.59°W	28	1991/05/30	13:17:43	6.2	68.1	ALASKA PENINSULA
42.19°N	125.65°W	11	1991/07/13	02:50:14	6.1	70.5	OFF COAST OF OREGON
50.65°N	130.06°W	10	1992/04/06	13:54:40	5.9	64.7	VANCOUVER ISLAND REGION
40.36°N	124.05°W	15	1992/04/25	18:06:04	6.2	71.5	NEAR COAST OF NORTHERN CALIFORNIA
40.51°N	124.25°W	20	1992/04/26	07:41:41	5.8	71.4	NEAR COAST OF NORTHERN CALIFORNIA
40.47°N	124.36°W	22	1992/04/26	11:18:26	6.4	71.5	NEAR COAST OF NORTHERN CALIFORNIA
34.25°N	116.48°W	1	1992/06/28	11:57:35	6.1	73.5	SOUTHERN CALIFORNIA
50.46°N	174.93°W	10	1992/08/19	00:57:40	6.0	73.5	ANDREANOF ISLANDS, ALEUTIAN IS.
43.94°N	128.33°W	20	1992/08/21	01:02:18	5.5	69.9	OFF COAST OF OREGON
59.66°N	152.97°W	108	1993/03/19	12:20:50	5.1	62.0	SOUTHERN ALASKA
56.26°N	155.01°W	25	1993/04/16	04:09:19	5.2	65.5	ALASKA PENINSULA
55.00°N	160.39°W	32	1993/05/13	11:59:47	6.3	67.6	ALASKA PENINSULA
55.01°N	160.56°W	30	1993/05/25	23:16:42	6.2	67.6	ALASKA PENINSULA
50.18°N	177.45°W	3	1993/11/11	00:28:31	6.2	73.9	ANDREANOF ISLANDS, ALEUTIAN IS.
60.17°N	153.11°W	124	1993/11/20	19:24:51	5.6	61.5	SOUTHERN ALASKA
40.44°N	125.69°W	10	1994/09/01	15:15:53	6.5	72.0	OFF COAST OF NORTHERN CALIFORNIA

Table 3. Data set statistics.

	NORSAR	Scotland
No. of events used	34	31
Average no. of picks per event	19.9	6.9
Total no. of picks	678	214

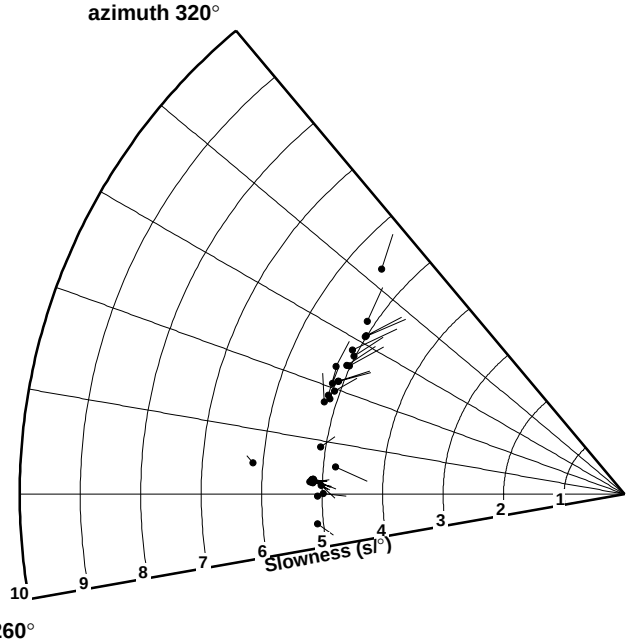

Figure 4. Slowness vectors observed at NORSAR for *P* phases from earthquakes in middle America, measured in this study. Dots: slownesses predicted from ISC hypocentres and the IASP91 earth model (Kennett & Engdahl 1991). Lines join these values to the observed slownesses.

near-array structure will introduce noise into the results (Berteussen 1975). Experiments using different sets of stations indicate that this effect is small (around $\pm 0.75^\circ$ in azimuth). We reduced the errors still further by applying station corrections to the observed times before fitting plane waves. The correction for each station is the average misfit between the predicted and observed times for all events. The overall effect of this correction is to reduce the noise in the results and to make measured azimuth anomalies more accurate.

RESULTS

NORSAR

The NORSAR misfits are plotted in slowness space in Fig. 4. The pattern observed is similar to that observed by Sheppard (1973). Waves from events due west of NORSAR arrive nearly from the great-circle azimuth, but waves from the northwest arrive from directions about 7° too far to the northwest. The same data are shown plotted in the form of azimuth anomalies as a function of azimuth in Fig. 5. This emphasizes the most important aspect of the data, because the primary effect of a vertical plume is to change the azimuthal component of the slowness vectors, while leaving the radial component little affected. The error bars are calculated assuming an aperture of 100 km for the NORSAR array and a maximum across-array picking error of 0.05 s, using the formula

$$\delta\zeta_\sigma = \tan^{-1}(\Delta\tau/pA),$$

where $\delta\zeta_\sigma$ is the error in azimuth anomaly, $\Delta\tau$ is the picking error, p is the slowness in s km^{-1} and A is the aperture. The slowness of the waves we study at NORSAR is $\sim$0.045 s km^{-1}, so the azimuth errors are about 0.64°.

The first-order feature of the results is a quasi-linear increase in the azimuth anomalies for azimuths between 270° and 300°. This linear trend is probably due to a very large-scale structure

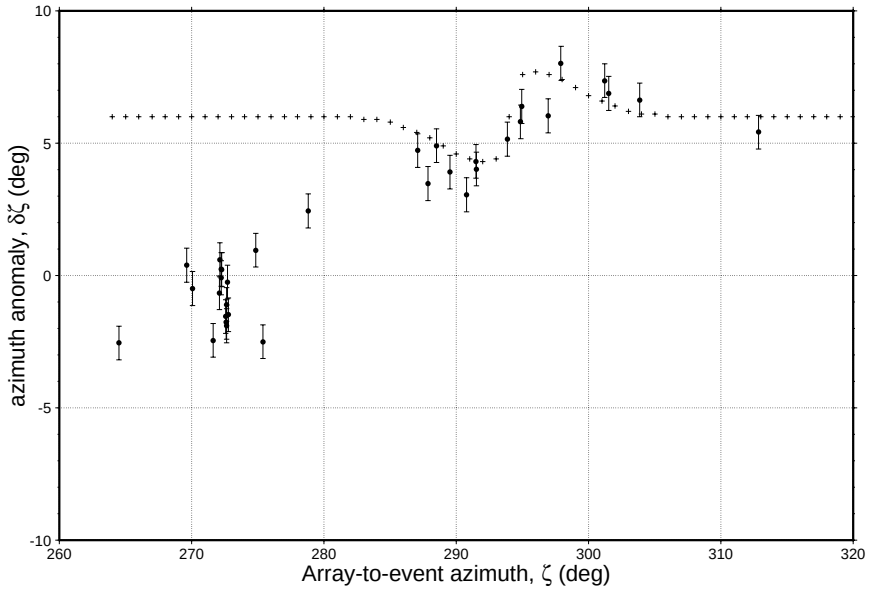

Figure 5. *P*-phase azimuth anomalies observed at NORSAR for the data shown in Fig. 4, along with error bars. Positive values indicate waves arriving from more northerly azimuths than the great circle to the epicentre. Also shown is the theoretical azimuth anomaly for an anomaly with a V_P contrast of 1.5 per cent and Gaussian diameter 250 km, shifted vertically to achieve the best fit to the observations.

somewhere west of NORSAR. A second-order feature occurs at azimuths of 290°–300° that has approximately the shape that would be expected if it were caused by a vertical, low-wave-speed plume. It is not possible to associate this feature with a plume unambiguously, but it is possible to use these observations to place bounds on the possible strength and size of a plume beneath the Iceland region.

Scotland

The observations from Scotland are shown in a similar way to the NORSAR data in Figs 6 and 7. The errors in Fig. 7 are calculated assuming an across-array picking error of 0.1 s and a network aperture of 100 km. The slowness of the wavefronts of the earthquakes we use is ~ 0.055 s km^{-1} and this yields an error in the azimuth anomalies of 1°. The scatter in the Scottish data is very large because of the poorer quality of the arrival-time measurements. The magnitude of the scatter, in fact, suggests that the official picking accuracy of 0.1 s for these data may be an underestimate, and that twice this, or about 0.2 s, might be more realistic.

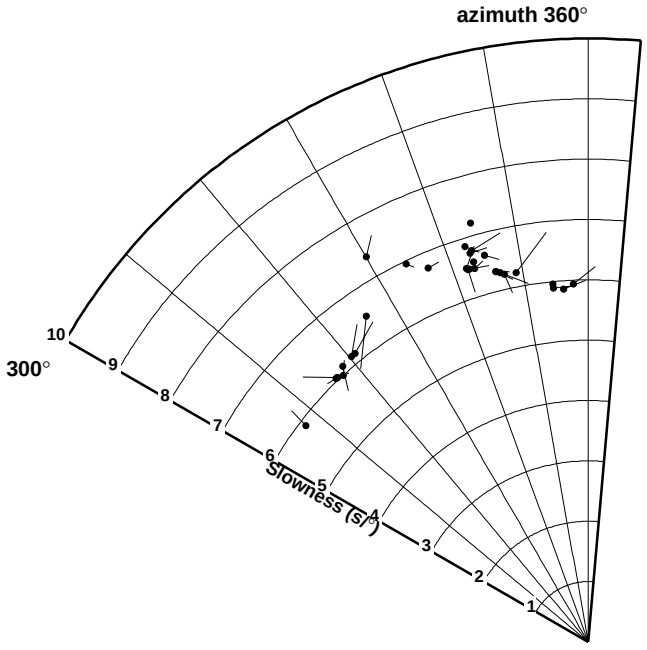

Figure 6. As Fig. 4 except for the Scottish data.

INTERPRETATION

Plume model

We approximate a plume as a vertical cylinder with low wave-speed V_P using the simple analytical function

$$V_P = V_0 - \delta V \exp(-r^2/a^2), \tag{1}$$

where r is distance from the plume axis, V_0 is the wave speed far from the plume, δV is the maximum wave-speed perturbation, and a, the 'Gaussian radius', is the distance at which the perturbation falls to $\delta V/\mathrm{e}$. No vertical variation is included. The horizontal wave-speed gradient near the plume refracts rays horizontally, causing them to arrive from azimuths different from those of the great circles to the epicentres. If the radius of the plume, a, is small compared with the epicentral distance, and if $\delta V \ll V_0$, so that the total deviation of the ray is much less than a radian, then on dimensional grounds the azimuth anomaly caused by the plume is

$$\delta\zeta \approx \left[1 - \frac{\Delta_\mathrm{p}}{\Delta}\right] \frac{\delta V}{V_0} f\left(\frac{(\zeta - \zeta_\mathrm{p})\Delta_\mathrm{p} R_\mathrm{E}}{a}\right), \tag{2}$$

where Δ is the (angular) epicentral distance, Δ_p is the distance from the array to the plume, ζ is the great-circle azimuth from the array to the epicentre, ζ_p is the azimuth from the array to the centre of the plume, R_E is the radius of the Earth, and f is a function that depends on the form of the wave-speed anomaly. In other words, the azimuth anomaly, as a function of azimuth,

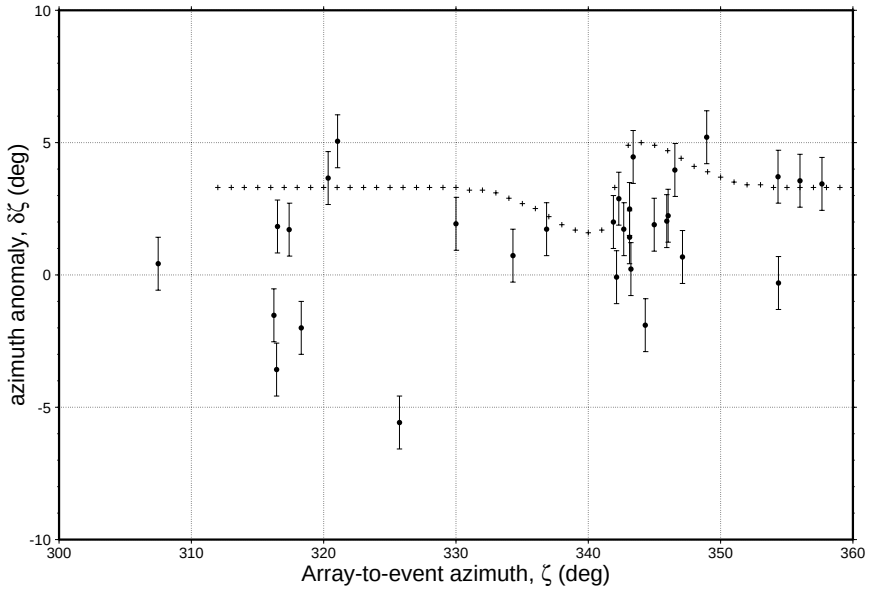

Figure 7. As Fig. 5 except for the Scottish data.

has a characteristic shape, with an amplitude proportional to the fractional wave-speed perturbation associated with the plume, and to the fraction of the path length that lies between the epicentre and the plume, and a width proportional to the angle subtended by the plume at the array. From symmetry considerations, f is an odd function. We determined the shape of f for the Gaussian anomaly of eq. (1) by numerical ray tracing using the bending method (Julian & Gubbins 1977). The results are shown in Fig. 8.

Comparison with the data

A theoretical azimuth-anomaly curve is superimposed on the NORSAR data in Fig. 5. The position of the anomaly has been placed at the approximate location of the low-wave-speed body observed beneath the Iceland–Faeroe ridge at a depth of ~700–1500 km by whole-mantle tomography (Bijwaard & Spakman 1999). The width of the anomaly has been chosen to fit the data. The amplitude of the anomaly has been made as large as is consistent with the data and thus provides an upper bound on the V_P anomaly of the causative body. The anomaly is centred at an azimuth of 295°, has a width of ~20°, and an amplitude of ~4°. These values correspond to a relative wave-speed perturbation in a plume, $\delta V/e$, of 1.5 per cent, and a plume Gaussian diameter, $2a$, of 250 km.

A similar curve is superimposed on the Scottish data in Fig. 7. The diameter and wave-speed perturbation are the same as those used for Fig. 5. The curve is centred at an azimuth of 342°, the approximate azimuth of the low-wave-speed body beneath the Iceland–Faeroe ridge. The scatter in the Scottish data is too great to resolve a feature of the same amplitude as detected in the NORSAR data. The backazimuths 295° from NORSAR and 342° from Scotland are plotted in Fig. 9.

DISCUSSION AND CONCLUSIONS

Recent whole-mantle tomography has cast light on the large-scale wave-speed structures beneath the Iceland region (Bijwaard & Spakman 1999; Bijwaard *et al.* 1998; Ritsema *et al.* 1999; Megnin & Romanowicz 2000). In the lowermost mantle, wave speeds beneath Newfoundland are generally high. At mid-mantle depths, a weak, low-wave-speed body is imaged beneath the Iceland–Faeroe ridge, southeast of Iceland, in the depth range 700–1500 km. This anomaly broadens and extends westwards with depth and underlies Greenland in the depth range 2000–2500 km.

Anomalies in the arrival directions of teleseismic P waves recorded at NORSAR are consistent with the existence of a vertical, cylindrical, low-wave-speed body with a V_P anomaly of ~1.5 per cent and a Gaussian diameter of ~250 km at a depth of ~1500 km beneath the Iceland–Faeroe ridge. The NORSAR data alone cannot uniquely determine the location of this possible plume, but only its direction from southern Norway. Data from seismic stations in Scotland are potentially capable of resolving this ambiguity, but the data analysed in this study are of inadequate quality. The abrupt, short-wavelength feature seen from the azimuth of the Iceland–Faeroe ridge is unique in the NORSAR data. Variations in azimuth anomaly at NORSAR do occur in other directions, for example at an azimuth of ~60° (from the Chinese–Russian border region), but they are broader and less extreme (Sheppard 1973). It would be interesting to study these anomalies also, although they may not be modelled well by plume-like structures.

There is a trade-off between the distance of the causative body from NORSAR and its size. We searched parameter space by modelling a suite of vertical cylinders with various strengths

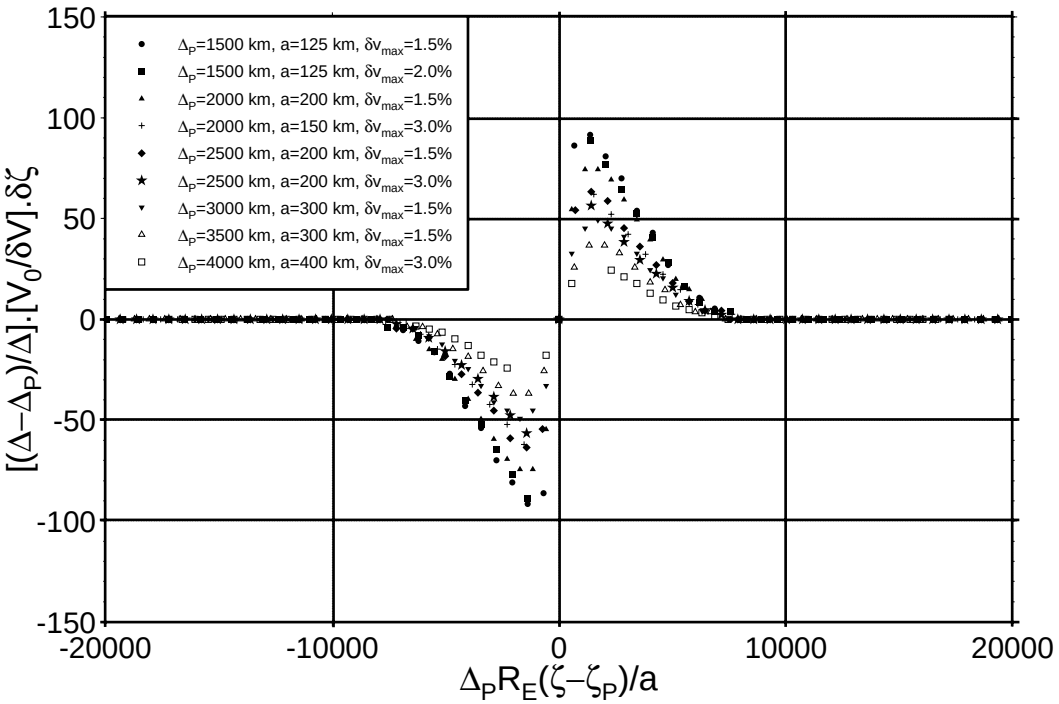

Figure 8. Theoretical azimuth anomalies for vertical plumes with various distances, Gaussian diameters and wave-speed perturbations (eq. 1), plotted in dimensionless form. The abscissa is the dimensionless difference between the great-circle azimuth to the epicentre and the azimuth to the plume. The ordinate is the dimensionless azimuth anomaly caused by the plume.

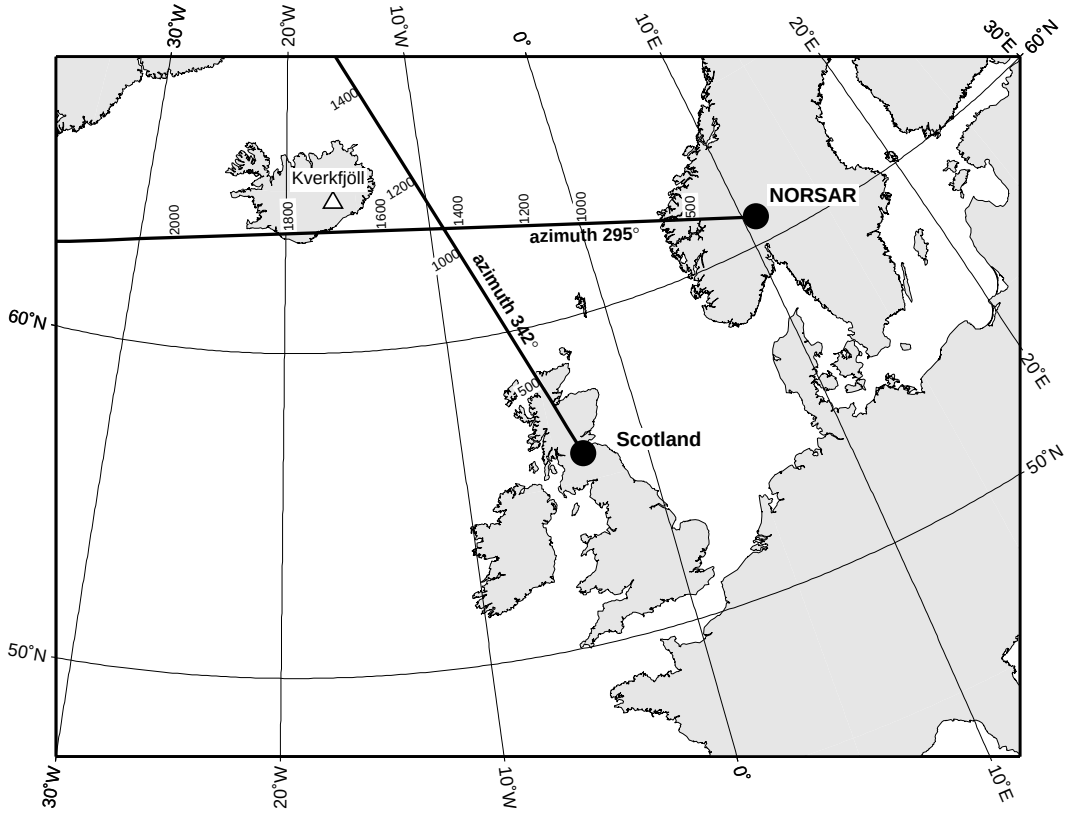

Figure 9. Map showing the surface projection of the best array-to-anomaly azimuth deduced from modelling of the NORSAR data. The azimuth of 342° plotted from the Scottish network passes through the low-wave-speed body imaged beneath the Iceland–Faeroe ridge by Bijwaard & Spakman (1999) using whole-mantle tomography. Depth annotations show the depth of penetration of waves in km.

and widths at various distances. Bodies with V_P anomalies up to a few per cent would have to be wider and deeper if more distant from NORSAR, reaching a diameter of 650 km at 3000 km distance (i.e. beneath Greenland) and 800 km at 4000 km distance (i.e. beneath Newfoundland). Broader, deeper bodies more distant than the Iceland–Faeroe ridge could thus also explain our observations, and the low-wave-speed body imaged by whole-mantle tomography beneath Greenland is a candidate. The complexity of the low-wave-speed region imaged by whole-mantle tomography makes it clear that our vertical, cylindrical plume model is a simplification.

Although the location of the causative body responsible for the anomaly at NORSAR cannot be determined unambiguously, the observations can place an upper limit on the magnitude of a possible plume in the mid-lower mantle beneath the Iceland–Faeroe ridge. Such a plume cannot be wider than $\sim$250 km and cannot have a V_P contrast of more than $\sim$1.5 per cent. A wider plume would produce a broader anomaly at NORSAR, and a stronger plume would produce a greater anomaly amplitude. A plume that is not vertical would present an aspect to arriving waves that is wider than its axis-normal diameter, and thus could be narrower than 250 km. The size and strength of the low-wave-speed body imaged by whole-mantle tomography is $\sim$500 km in diameter and up to $\sim$0.5 per cent. The discrepancy with our results is consistent with the fact that whole-mantle tomography has relatively low resolution, and small, strong anomalies tend to be imaged as broader, weaker anomalies. Our results suggest that this may be the case for the low-wave-speed bodies imaged in the lower mantle beneath the Iceland region.

ACKNOWLEDGMENTS

Help with data collection from Ulf Baadshaug at the NORSAR Data Processing Centre, Kjeller, Norway, and Davie Galloway and Paul Henni at BGS, Edinburgh is gratefully acknowledged. The figures were produced using the GMT plotting package of Wessel & Smith (1991). This paper was greatly improved by detailed, critical reviews by two anonymous reviewers. Any use of trade, product, or firm names is for descriptive purposes only and does not imply endorsement by the US Government.

REFERENCES

Allen, R.M. *et al.*, 1998. The thin hot plume beneath Iceland, *Geophys. J. Int.,* **137,** 51–63.

Anderson, D.L., 1998a. The helium paradoxes, *Proc. Natl Acad. Sci. USA,* **95,** 4822–4827.

Anderson, D.L., 1998b. A model to explain the various paradoxes associated with mantle noble gas geochemistry, *Proc. Natl Acad. Sci. USA,* **95,** 9087–9092.

Anderson, D.L. 1993. Helium-3 from the mantle: primordial signal or cosmic dust?, *Science,* **261,** 170–176.

Berteussen, K.A., 1975. Array analysis of lateral inhomogeneities in the deep mantle, *Earth. planet. Sci. Lett.,* **28,** 212–216.

Bijwaard, H. & Spakman, W., 1999. Tomographic evidence for a narrow whole mantle plume below Iceland, *Earth planet. Sci. Lett.,* **166,** 121–126.

Bijwaard, H., Spakman, W. & Engdahl, E.R., 1998. Closing the gap between regional and global travel time tomography, *J. geophys. Res.,* **103,** 30 055–30 078.

Bondar, I., North, R.G. & Beall, G., 1999. Teleseismic slowness-azimuth station corrections for the international monitoring system seismic network, *Bull. seism. Soc. Am.,* **89,** 989–1003.

Buland, R. & Chapman, C.H., 1983. The computation of seismic travel times, *Bull. seism. Soc. Am.,* **73,** 1271–1302.

Bungum, H., Husebye, E.S. & Ringdal, F., 1971. The NORSAR array and preliminary results of data analysis, *Geophys. J. R. astr. Soc.,* **25,** 115–126.

Fitton, J.G., Saunders, A.D., Norry, M.J., Hardarson, B.S. & Taylor, R.N., 1997. Thermal and chemical structure of the Iceland plume, *Earth. planet. Sci. Lett.,* **153,** 197–208.

Foulger, G.R. *et al.*, 2000. The seismic anomaly beneath Iceland extends down to the mantle transition zone and no deeper, *Geophys. J. Int.,* **142,** F1–F5.

Helmberger, D.V., Wen, L. & Ding, X., 1998. Seismic evidence that the source of the Iceland hotspot lies at the core–mantle boundary, *Nature,* **396,** 251–255.

Ji, Y. & Nataf, H.-C., 1998. Detection of mantle plumes in the lower mantle by diffraction tomography: Hawaii, *Earth. planet. Sci. Lett.,* **159,** 99–115.

Julian, B.R. & Gubbins, D., 1977. Three-dimensional seismic ray tracing, *J. geophys. Res.,* **43,** 95–113.

Kennett, B.L.N. & Engdahl, E.R., 1991. Traveltimes for global earthquake location and phase identification, *Geophys. J. Int.,* **105,** 429–465.

Megnin, C. & Romanowicz, B., 2000. The three-dimensional shear velocity structure of the mantle from the inversion of body, surface and higher mode waveforms, *Geophys. J. Int.,* in press.

Morgan, W.J., 1971. Convection plumes in the lower mantle, *Nature,* **230,** 42–43.

Nataf, H.-C. & VanDecar, J., 1993. Seismological detection of a mantle plume?, *Nature,* **364,** 115–120.

Richards, M.A., Hager, B.H. & Sleep, N.H., 1988. Dynamically supported geoid highs over hotspots: observation and theory, *J. geophys. Res.,* **93,** 7690–7708.

Ritsema, J., van Heijst, H.J. & Woodhouse, J.H., 1999. Complex shear wave velocity structure imaged beneath Africa and Iceland, *Science,* **286,** 1925–1928.

Shen, Y., Solomon, S.C., Bjarnason, I.Th. & Purdy, G.M., 1996. Hot mantle transition zone beneath Iceland and the adjacent mid-Atlantic ridge inferred from P-to-S conversions at the 410- and 660-km discontinuities, *Geophys. Res. Lett.,* **23,** 3527–3530.

Shen, Y., Solomon, S.C., Bjarnason, I.Th. & Wolfe, C.J., 1998. Seismic evidence for a lower mantle origin of the Iceland plume, *Nature,* **395,** 62–65.

Sheppard, R.M., 1973. NORSAR array mislocations, in *Seismic Discrimination, Semiannual Technical Summary,* pp. 12–13, Lincoln Laboratory, Lexington, MA.

Tryggvason, K., Husebye, E.S. & Stefánsson, R., 1983. Seismic image of the hypothesized Icelandic hot spot, *Tectonophysics,* **100,** 94–118.

van der Hilst, R.D., Widiyantoro, S. & Engdahl, E.R., 1997. Evidence for deep mantle convection from global tomography, *Nature,* **386,** 578–584.

Wessel, P. & Smith, W.H.F., 1991. Free software helps map and display data, *EOS, Trans. Am. geophys. Un.,* **72,** 441, 445–446.

Wolfe, C.J., Bjarnason, I.T. & Solomon, S.C., 1997. Seismic structure of the Iceland plume, *Nature,* **385,** 245–247.